Hindawi Publishing Corporation
Journal of Nanotechnology
Volume 2015, Article ID 614170, 8 pages
http://dx.doi.org/10.1155/2015/614170

Research Article

Preparation of ZnO/CdS/BC Photocatalyst Hybrid Fiber and Research of Its Photocatalytic Properties

Beibei Dai, Cheng Chao, Xiaoyu Lu, Qingcheng Xia, Jing Han, Fei Mao, Jiazhi Yang, and Dongping Sun

Chemicobiology and Functional Materials Institute, Nanjing University of Science and Technology, Nanjing 210094, China

Correspondence should be addressed to Jiazhi Yang; jzhyangb504@163.com

Received 6 May 2015; Revised 3 July 2015; Accepted 9 July 2015

Academic Editor: Enkeleda Dervishi

An environment-friendly biomaterial bacterial cellulose (BC) is introduced to substitute general organic polymers to assist the preparation of ZnO/CdS/BC photocatalyst hybrid nanofiber through coprecipitation method under the low-temperature condition. The XRD, XPS, and SEM results show that high load of ZnO/CdS/BC ternary hybrid fiber can be produced. TGA curves scan shows that ZnO/CdS/BC hybrid fiber has better thermal properties than bacterial cellulose. The UV-Vis spectra of the ZnO/CdS/BC hybrid nanofiber (0, 10, 20, and 50 wt%, resp.) show that photocatalytic activities of ZnO/CdS/BC are influenced by the added amount of CdS. The degradation curve of methyl shows that ZnO/CdS/BC nanohybrid fibers exhibit excellent photocatalytic efficiency.

1. Introduction

Zinc oxide (ZnO) is deemed to be one of the most important photocatalysts because of its high photosensitivity, nontoxicity, and great stability [1–5]. However, it is known that ZnO could not effectively absorb and utilize the visible region of the solar light, because of the fast recombination of the photogenerated electron hole pairs in the single phase semiconductor [6, 7]. CdS, as a representative II–VI compound semiconductor, has been used as a visible-light photocatalyst [8] and also as a photosensitizer of various wide band-gap semiconductor photoanodes in photoelectrochemical cells due to its narrow direct band-gap (2.4 eV) [9]. However, it is very easy etching, resulting in the decreased service life [10, 11]. The combined ZnO and CdS system in nanosize area has attracted a great deal of attention in recent years. It can enhance the photocatalytic efficiency of ZnO under visible light and the service life of CdS, due to the fast separation of the photogenerated electron hole pairs [12–17].

However, there are disadvantages such as the aggregation and the bleeding of the photocatalyst of the CdS/ZnO suspended photocatalyst. It can be overcome through the photocatalyst fixation instead of the recovery of the photocatalyst [10–20]. The key of immobilized technique is the performance of adopted immobilized carriers. Selection of carriers for supported CdS/ZnO suspended photocatalyst was systematically studied in earlier reports. Glass cloth, activated carbon, refractory brick, sand particle, hollow glass beads, ceramic, silica, and so forth are common catalyst supporters with broad application potentials [19]. However, the absorption and activity of catalyst could be decreased by using such supporter for immobilization of catalyst due to their low specific surface area and nonhomogeneous porosity. In order to improve the performance of the catalyst, nanometer fiber/nanotubes as the catalyst supporters have been conducted recently. As a new kind of materials, nanometer fiber/nanotubes carriers have attracted considerable interest because of their unique structural, mechanic, electronic, and potential applications [21].

Cellulose is one of the most abundant natural resources. Bacterial cellulose (BC) fiber produced by *Acetobacter xylinum* is considered as a cleaner sustainable biomaterial and attracts much attention due to its remarkable advantages of good mechanic properties, good chemical stability, high purity, high specific surface area, high crystallinity, great compatibility, and being environmentally friendly [22]. The diameter of BC fiber is common of 10–100 nm. It has been found that biomaterials were widely used as

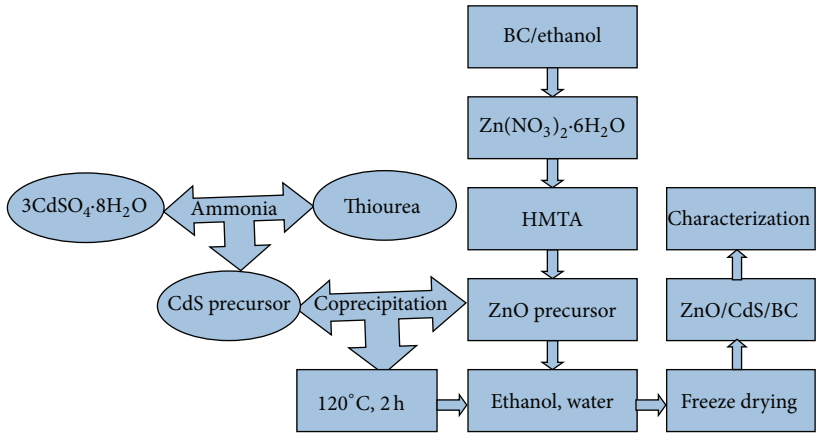

Figure 1: Schematic preparation process of hybrid ZnO/CdS/BC fibers.

a template in the synthesis of various inorganic nanostructures. Various methods have been reported for the synthesis of ZnO/CdS nanorods including colloidal chemical synthesis [16], electrochemical deposition [23], chemical bath deposition technique [24], facile chemical route [25], combined sol-gel/hydrothermal/SILAR method [26], chemical precipitation method [27], and sonochemical synthesis [28]. Among these methods, coprecipitation process is a simple and low-cost method that can be performed at low temperature and ambient pressure.

In this study, we used BC as template to prepare ZnO/CdS/BC ternary hybrid fiber. The samples were characterized by X-ray diffraction (XRD), scanning electron microscopy (SEM), thermogravimetric analysis (TGA), X-ray photoelectron spectra (XPS), UV-Vis absorption spectroscopy (UV-Vis), and the photocatalytic activity measurements. This study would provide a new type of nanofiber photocatalysis materials. It also opened up a new field of potential applications of BC materials.

2. Experimental

2.1. Materials. Bacterial cellulose (BC) was biosynthesized by *Acetobacter xylinum* NUST5.2. The cadmium sulfate octahydrate ($3CdSO_4{\cdot}8H_2O$) was purchased from Guangdong Company (Guangdong, China). Analytical-grade sodium hydroxide (NaOH), zinc nitrate hexahydrate ($Zn(NO_3)_2{\cdot}6H_2O$), hexamethylenetetramine (HMTA), ethanol (C_2H_5OH), ammonia water ($NH_3{\cdot}H_2O$), dibasic sodium phosphate (Na_2HPO_4), glucose ($C_6H_{12}O_6$) were purchased from Sinopharm Chemical Reagent Co., Ltd. All aqueous solutions were prepared with deionized water produced by laboratory water purification system. All other chemicals were analytical reagent unless stated otherwise.

2.2. Preparation of BC Fibers. The pristine BC substrate was synthesized and purified as reported [29]. BC fibers were purified by soaking in DI at 70°C for 3 h and then 4 wt% NaOH in DI at 80°C for 180 min. Samples were then rinsed with DI to pH = 7 and stored in refrigerator at 4°C prior to use.

2.3. Preparation of Hybrid ZnO/CdS/BC Fibers. Figure 1 showed the preparation process of hybrid ZnO/CdS/BC fibers. In a typical procedure, the BC fibers were immersed in the ethanol solution with certain concentrations under magnetic stirring. Then, the BC fibers were dipped into an ethanol solution containing 0.5 g zinc nitrate hexahydrate [$Zn(NO_3)_2{\cdot}6H_2O$] with mechanical stirring (200 rpm) at 30°C for 10 h. Subsequently, hexamethylenetetramine (HMTA) was added into the above solvent and treated with ultrasonic for 1 h. Finally, different amounts of cadmium sulfate octahydrate [$3CdSO_4{\cdot}8H_2O$] (0.01 g/mL) solution including 5 mL, 10 mL, and 25 mL were added to the above as-prepared ZnO solution and labeled as 10 wt% ZnO/CdS/BC, 20 wt% ZnO/CdS/BC, and 50 wt% ZnO/CdS/BC, respectively. The mixture was stirred at 120°C temperature for another 12 h. The products were washed with distilled water and ethanol for several times to remove the possible residues and were dried in vacuum at 50°C for 24 h. After the reaction, the white solution turned light yellow with the CdS content increasing, indicating the formation of hybrid ZnO/CdS/BC fibers.

2.4. Characterization of Samples. The X-ray diffraction patterns (XRD) were recorded on a Bruker D8 ADVANCE X-ray diffractometer equipped with graphite monochromatized high-intensity CuKα radiation (λ = 0.15418 nm). Scanning electromicroscopy (SEM) images were performed on JSM-6380LV to obtain the morphology of the samples. The UV-visible spectra were recorded on a Cary 5000 spectrophotometer equipped with an integrated sphere accessory for diffusive reflectance spectra. Thermogravimetric analyses (TGA) were performed on a Boyuan DTU-2C thermogravimetric analyzer from 50 to 800°C at a heating rate of $10^{\circ}C{\cdot}min^{-1}$ in air flow. High resolution XPS and wide XPS spectra were achieved to investigate the composition and chemical states of the samples. X-ray photoelectron

spectra (XPS) were carried out on a RBD upgraded PHI-5000C ESCA system (Perkin Elmer) with Mg Kα radiation ($h\nu$ = 1253.6 eV). The XPS peaks were deconvoluted using Lorentzian-Gaussian components after a Shirley background subtraction.

2.5. Photocatalytic Activity Measurements. The photocatalytic activities of the samples were evaluated by photodegradation of the methyl orange under a simulated sunlight from a 500 W Xe lamp at room temperature. The reaction suspensions formed by 20 mg ZnO/CdS/BC hybrid nanofiber (10%) and 40 mL methyl orange (20 mg/L). Prior to irradiation, the suspensions were stirred in the dark for 30 min to achieve the adsorption/desorption equilibrium. After a given irradiation time, a small amount of the solution was withdrawn for analysis of the methyl orange concentration after centrifuging. The photodegradation of the methyl orange solution was investigated by measuring its absorbance by the UV-Vis spectrophotometer (Evolution 220) at the maximum absorption around λmax = 500 nm. A good linear relationship between the concentration and absorbance at low concentration is presented according to Lambert-Beer's law:

$$\eta = \frac{C_0 - C_t}{C_0} \times 100\% = \frac{A_0 - A_t}{A_0} \times 100\%, \quad (1)$$

where C_0 is the initial concentration of methyl orange solution, A_0 means the initial absorbance, C_t is the concentration at the t moment, and A_t is the concentration at the moment.

3. Results and Discussion

3.1. X-Ray Diffraction Patterns (XRD). The XRD patterns of bacterial cellulose, pure ZnO, and ZnO/BC hybrid fiber are described in Figure 2. Figure 2(a) shows the pronounced diffraction peaks with $2\theta = 14.5^\circ, 16.6^\circ$, and 22.5° corresponding to the (101), (10$\bar{1}$), and (002) planes of the BC fibers [22]. Figure 2(c) shows the peaks of pure ZnO nanorod. It indicates that the presence of ZnO nanorod attributes to peaks at $2\theta = 31.8^\circ, 34.4^\circ, 36.3^\circ, 47.5^\circ, 56.6^\circ, 62.9^\circ, 66.4^\circ, 68.0^\circ$, and 69.1°. These are associated with the (100), (002), (101), (102), (110), (103), (200), (112), and (201) planes of the ZnO hexagonal wurtzite structure [9]. Figure 2(b) shows XRD patterns of ZnO/BC hybrid nanofiber. It can be seen that all diffraction peaks could be identified to BC fibers and ZnO peaks with hexagonal wurtzite structure. No other peaks related to impurities are detected in the pattern which further confirms that the synthesized hybrid nanofibers were BC and single phase of ZnO with hexagonal wurtzite structure. Meanwhile, three characteristic peaks located at 14.5°, 16.6°, and 22.5° from BC fibers are weakened due to a lot of nanorods wrapped on the surface of BC fibers.

Figure 3 presents the XRD patterns of the ZnO/CdS/BC hybrid fiber. There are two sets of diffraction peaks for ZnO/CdS/BC nanoheterostructure, which can be ascribed to hexagonal wurtzite ZnO and cubic CdS, respectively. In contrast to the standard diffraction peaks (JCPDS number 36-1451), the pronounced and high diffraction peaks with

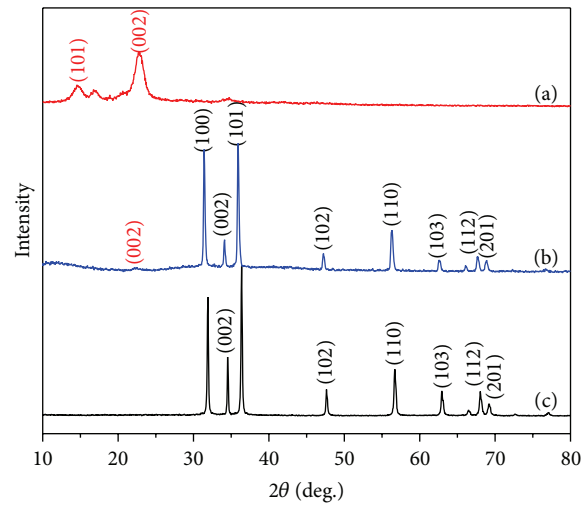

Figure 2: XRD patterns of (a) bacterial cellulose, (b) ZnO/BC hybrid fiber, and (c) ZnO.

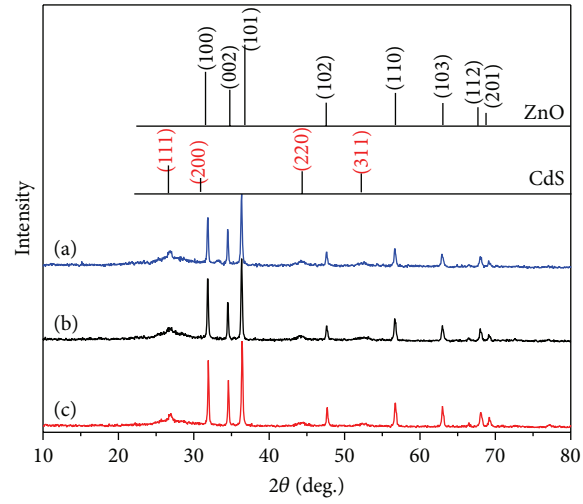

Figure 3: XRD patterns of (a) ZnO/CdS/BC hybrid fiber (50%), (b) ZnO/CdS/BC hybrid fiber (20%), and (c) ZnO/CdS/BC hybrid fiber (10%).

2θ = 31.8°, 34.4°, 36.3°, 47.5°, 56.6°, 62.9°, 66.4°, 68.0°, and 69.1° correspond to the (100), (002), (101), (102), (110), (103), (200), (112), and (201) planes of the hexagonal ZnO, respectively [9]. Meanwhile, broader and weaker diffraction peaks with 2θ = 26.5°, 43.9°, and 52.0° are observed and they are found to be consistent with those of the standard CdS (JCPDS number 89-0440), corresponding to the (111), (220), and (311) planes of the CdS, respectively, suggesting the existence of ZnO and CdS [8]. And the ZnO diffraction peaks get weaker with increasing contents of CdS. It implies the highly crystalline character of ZnO and the little crystal size of CdS in the sample.

3.2. Scanning Electron Microscopy (SEM). The morphologies of BC and ZnO/CdS/BC hybrid nanofiber (10, 20, and 50 wt%, resp.) structure are investigated by SEM.

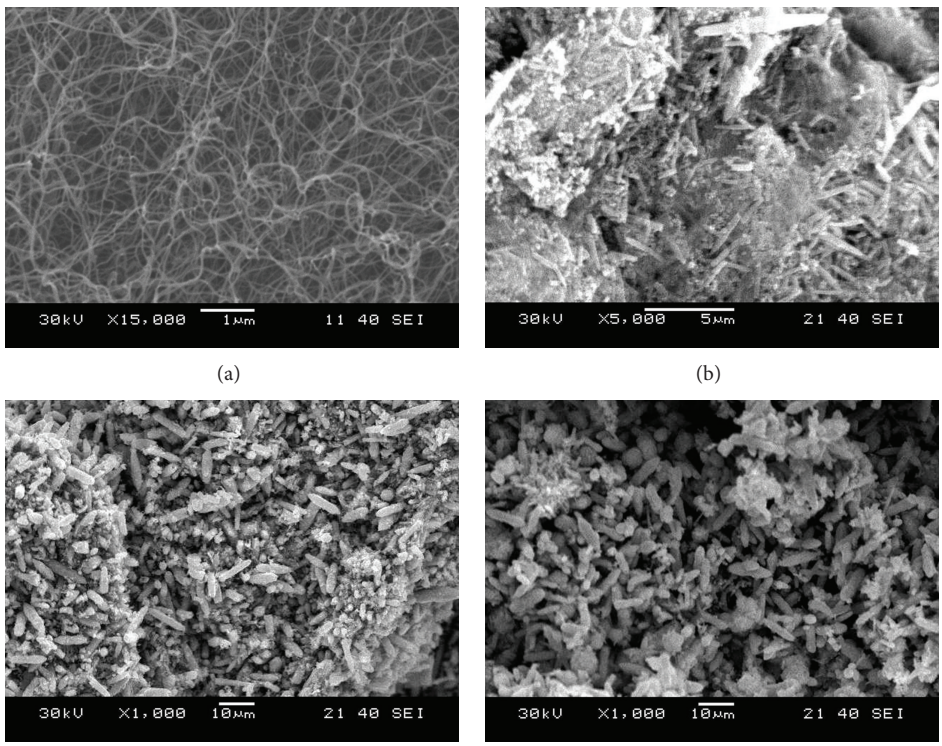

Figure 4: (a) SEM of bacterial cellulose and ((b)–(d)) samples prepared at 120°C with CdS contents at 10%, 20%, and 50%.

Figure 4(a) shows SEM images of bacterial cellulose nanofibers biosynthesized by *Acetobacter xylinum* NUST 5.2. It presents a three-dimensional network structure with an average diameter of about 30 nm. The three-dimensional network structure contains a lot of lone pair electrons in the hydroxyl groups, which play an active role in anchoring the nanoparticles. Figure 4(b) shows SEM images of ZnO/CdS/BC (10%) nanoheterostructure, there are many nanoparticles with the sizes of several nanometers growing on the surfaces of the hybrid fiber, and the particle has a spherical shape. The surfaces become coarse compared with those of ZnO nanorods. Figure 4(c) shows SEM images of ZnO/CdS/BC (20%) nanoheterostructure. It clearly indicates that there are a large number of CdS nanoparticles growing on the surfaces and the surrounding of the hybrid fiber. The SEM of the ZnO/CdS/BC hybrid nanofiber (50 wt%) is shown in Figure 4(d). It is found that the whole hybrid fiber was coated by CdS nanoparticles. Therefore, the formation of hybrid ZnO/CdS/BC fibers was established.

3.3. Thermogravimetric Analysis (TGA). Thermal stability of the polymer films was examined at the temperature range of 50–800°C with a heat in grate of 10°C/min, under nitrogen flushed at 200 mL/min using Boyuan DTU-2C thermogravimetric analyzer. As the temperature increased, a graph of weight loss (%) versus temperature was plotted. Bacterial cellulose and ZnO/CdS/BC hybrid fiber (50%) were subjected to TGA to determine the thermal stability and decomposition characteristics.

Figure 5 shows TGA curves of bacterial cellulose and ZnO/CdS/BC hybrid fiber (50%). The TGA curve of bacterial cellulose shows one main weight loss stage ranging from 280°C to 380°C followed by the final decomposition of the polymer, which can be attributed to the decomposition of main chain of the polymers. At higher heating temperatures, the BC continues to decompose until about 99.8% was lost at temperatures above 600°C. However, only 22% weight was lost when the ZnO/CdS/BC hybrid fibers (50%) were decomposed at 600°C. TGA curves scan indicates that ZnO/CdS/BC hybrid fiber has better thermal properties than BC because ZnO/CdS/BC hybrid fiber does not completely lose weight at the temperature range. It can also indicate there is an interaction between BC and ZnO/CdS nanorod. It was evident that high load of ZnO/CdS/BC ternary hybrid fiber can be achieved in coprecipitation method, which agrees with the results from the latter X-ray photoelectron spectroscopy (XPS).

3.4. X-Ray Photoelectron Spectroscopy (XPS). High resolution XPS and wide XPS spectra are conducted to investigate the composition and chemical states of samples. Figure 6 shows the survey spectrum of the ZnO/CdS/BC hybrid fiber (50%). The Zn, O, Cd, C, and S peaks can be clearly observed in the survey spectrum. Carbon might come from the original

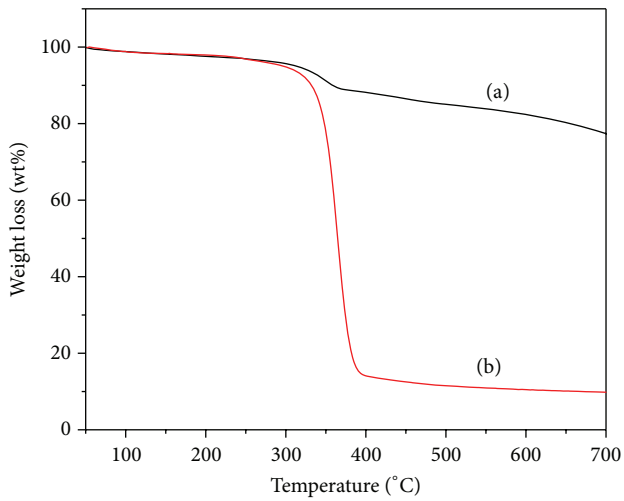

Figure 5: TG spectra of (a) ZnO/CdS/BC hybrid fiber (50%) and (b) bacterial cellulose.

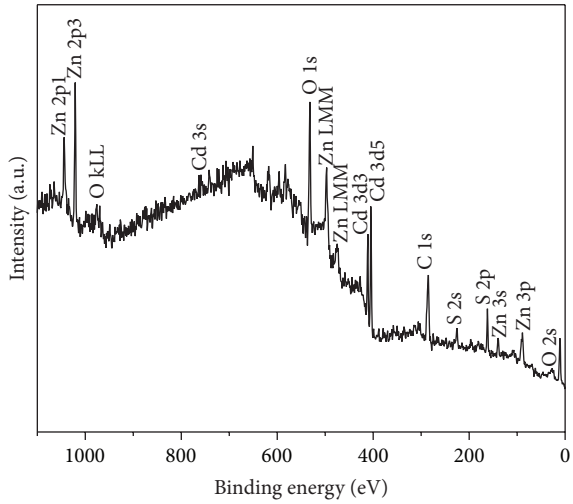

Figure 6: XPS of ZnO/CdS/BC hybrid fiber (50%).

source such as bacterial cellulose. Cadmium, zinc, sulfur, and oxygen are expected from the chemical composition of CdS and ZnO.

The narrow spectrum of Cd (a), O (b), S (c), and Zn (d) elements in ZnO/CdS/BC hybrid fiber (50%) is given in Figure 7. Figure 7(a) shows the multiplex spectrum of cadmium peaks. The peaks at binding energies of 411.9 eV and 404.7 eV can be assigned to Cd 3d3/2 and Cd 3d5/2 of Cd-S bond, respectively [30]. This is consistent with the binding energies reported in the literature [31, 32]. Figure 7(b) shows the multiplex spectrum of oxygen peaks. The peaks at binding energies of 539 eV can be assigned to O 1s [33]. In addition, Figure 7(c) shows the multiplex spectrum of sulfur peaks. The peaks at binding energies of 161.2 eV can be assigned to S 2p [34]. Figure 7(d) shows the multiplex spectrum of zinc peaks. The peaks at binding energies of 1021.7 eV can be assigned to Zn 2p3/2 of the Zn-O bond [35]. Moreover, by calculating determination of the peak area of XPS curve, we can see that the atom ratio of Cd/Zn is about 1, which is close to that of the theoretical standard.

As a result, XPS analysis reveals that a large number of ZnO/CdS nanorods are wrapped on the surface of BC fibers, successfully. It implies that the ternary hybrid fiber can be prepared with coprecipitation method under the low-temperature condition.

3.5. UV-Vis Absorption Spectroscopy (UV-Vis). The strong absorption edge of pure ZnO nanorods occurs at the wavelength of 387 nm and their band-gaps can be estimated to 3.21 eV. Compared to the pure ZnO sample, the high absorption edge of pure CdS nanorods occurs at the wavelength of 551 nm and their band-gaps can be estimated to 2.25 eV. Although CdS has a stronger absorption than ZnO in visible light region, the easy occurrence of photochemical corrosion limited its application ranges and lifespan. Therefore, the optimized combined treatment is more effective in preventing photochemical corrosion from CdS and extending the range of spectral response from ZnO. Meanwhile, the efficiency of electron cavity separated is increased and the activity of catalysts is improved.

Figure 8 shows the UV-Vis spectra of the ZnO/CdS/BC hybrid nanofiber (0, 10, 20, and 50 wt%, resp.) under 120°C condition. It is interesting to note that, by increasing the percentage of CdS from 0 to 50%, the absorption is much higher, which can be ascribed to the larger amount of deposited CdS. Compared to the pure ZnO sample, the red shift of ZnO/CdS/BC hybrid nanofiber is becoming more and more obvious. The results indicate that enhancement of the absorption in the visible spectral range could improve the activity of catalysts obviously.

3.6. Photocatalytic Activity Measurements. To evaluate the photocatalytic activity of the samples, the photodegradation of the methyl orange was investigated under the simulated sunlight from a 500 W Xe lamp. In the experiment, 20 mg of photocatalyst was suspended in 40 mL of a 20 mg/L aqueous solution of methyl orange. Prior to irradiation, the suspensions were stirred in the dark for 30 min to achieve an adsorption/desorption equilibrium. And then the suspensions were added to photocatalytic reactor. We took a sample in 30 min. The sample was first naturally precipitated and the absorbance for the supernatant was determined.

The photodegradation curves of the samples under UV irradiation are given in Figure 9. A blank test (methyl orange without any catalyst) under irradiation exhibited little decrease in the concentration of methyl orange and its degradation percentage of methyl orange reaches only 12% at 90 min in Figure 9(a). ZnO/BC hybrid fibers as a photocatalyst, by contract, its degradation percentage of methyl orange reached 58% at 90 min in Figure 9(b). For ZnO/CdS, its degradation percentage of methyl orange reaches 90% at 90 min in Figure 9(c). However, for ZnO/CdS/BC nanohybrid fibers (10%) as a photocatalyst, the photodegradation of methyl orange reached nearly 100% after 90 min of the light irradiation in Figure 9(d). It is found that ZnO/CdS/BC

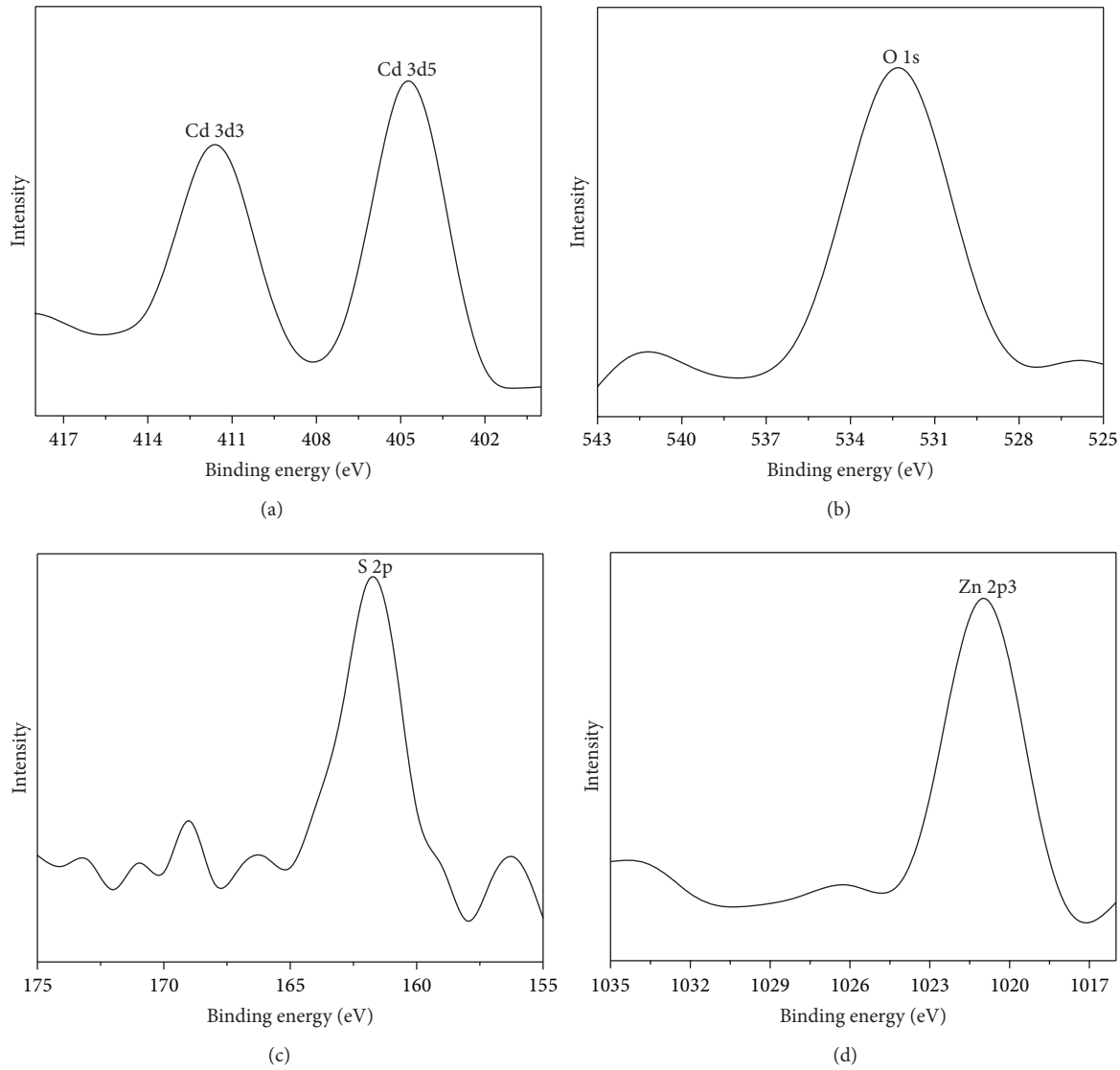

Figure 7: Narrow spectrum of (a) Cd, (b) O, (c) S, and (d) Zn, elements in ZnO/CdS/BC hybrid fiber (50%).

nanohybrid fibers (10%) show the best photocatalytic efficiency among the samples, which was mainly attributed to the extended photoresponding range toward visible light. Meanwhile, the BC has good fixation effects on ZnO/CdS nanoheterostructure; it provides greater specific surface area as well as more uniform morphology and helps reduce agglomeration.

4. Conclusions

In summary, an environment-friendly biomaterial bacterial cellulose (BC) was introduced to substitute general organic polymers to assist the preparation of ZnO/CdS/BC ternary hybrid fiber through coprecipitation method under the low-temperature condition. The XRD, XPS, and SEM results showed that high load of ZnO/CdS/BC ternary hybrid fiber could be produced. TGA curves scan revealed that ZnO/CdS/BC hybrid fiber had better thermal properties. The UV-Vis spectra of the ZnO/CdS/BC hybrid nanofiber (0, 10, 20, and 50 wt%, resp.) under 120°C condition indicated that photocatalytic activities of ZnO/CdS/BC were influenced by the added amount of CdS. It was noted that, by increasing the percentage of CdS from 0 to 50%, the absorption was more higher. Meanwhile, ZnO/CdS/BC nanohybrid fibers showed the best photocatalytic efficiency among the samples. In brief, the application of our ZnO/CdS/BC hybrid in photocatalysis would be promising because of its excellent photocatalytic performance and simple synthetic route.

Conflict of Interests

The authors declare that there is no conflict of interests regarding the publication of this paper.

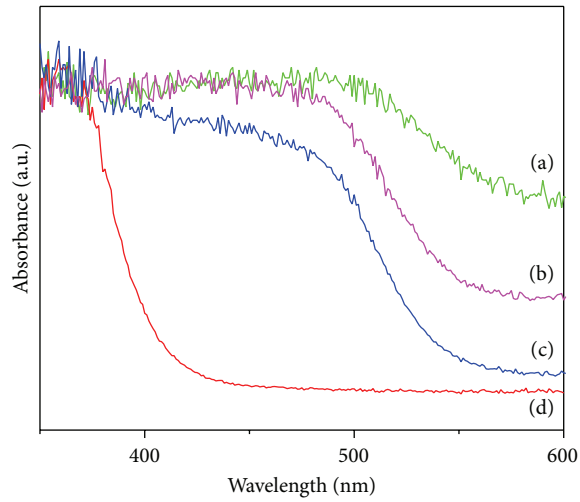

FIGURE 8: UV-Vis absorption spectrum of samples prepared at 120°C with CdS contents at 0, 10%, 20%, and 50%.

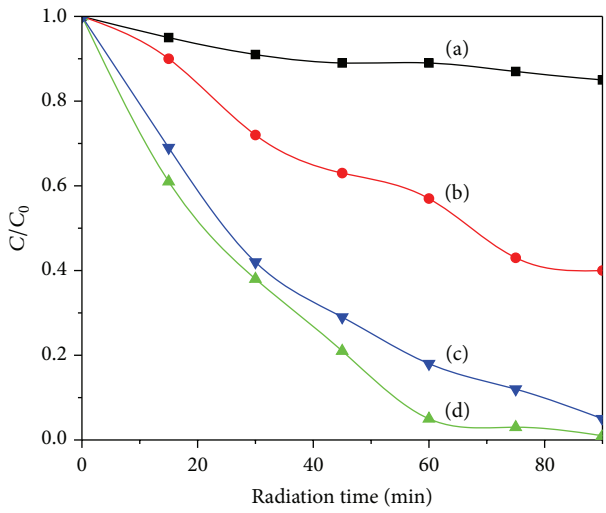

FIGURE 9: Degradation curve of methyl orange: (a) self-degradation of methyl orange, (b) ZnO/BC hybrid fibers, (c) ZnO/CdS, and (d) ZnO/CdS/BC hybrid fibers (10%).

Acknowledgments

The authors acknowledged the financial support from the National Natural Science Foundation of China (no. 21206076) and the Natural Science Foundation of Jiangsu Province (no. BK 2012401).

References

[1] F. Lu, W. P. Cai, and Y. Zhang, "ZnO hierarchical micro/nano-architectures: solvothermal synthesis and structurally enhanced photocatalytic performance," *Advanced Functional Materials*, vol. 18, no. 7, pp. 1047–1056, 2008.

[2] Y. Guo, H. S. Wang, C. l. He, L. J. Qiu, and X. B. Cao, "Uniform carbon-coated ZnO nanorods: microwave-assisted preparation, cytotoxicity, and photocatalytic activity," *Langmuir*, vol. 25, no. 8, pp. 4678–4684, 2009.

[3] R. Kitture, S. J. Koppikar, R. Kaul-Ghanekar, and S. N. Kale, "Catalyst efficiency, photostability and reusability study of ZnO nanoparticles in visible light for dye degradation," *Journal of Physics and Chemistry of Solids*, vol. 72, no. 1, pp. 60–66, 2011.

[4] X. Fang, Y. Bando, U. K. Gautam et al., "ZnO and ZnS nanostructures: ultraviolet-light emitters, lasers, and sensors," *Critical Reviews in Solid State and Materials Sciences*, vol. 34, no. 3-4, pp. 190–223, 2009.

[5] X. S. Fang and L. D. Zhang, "Controlled growth of one-dimensional oxide nanomaterials," *Journal of Materials Science and Technology*, vol. 22, no. 1, pp. 1–18, 2006.

[6] H. Herrmann, S. T. Martin, and M. R. Hoffmann, "Time-Resolved Radio Frequency Conductivity (TRRFC) studies of charge-carrier dynamics in aqueous semiconductor suspensions," *Journal of Physical chemistry*, vol. 99, no. 45, pp. 16641–16645, 1995.

[7] A. L. Linsebigler, G. Q. Lu, and J. T. Yates Jr., "Photocatalysis on TiO_2 surfaces: principles, mechanisms, and selected results," *Chemical Reviews*, vol. 95, no. 3, pp. 735–758, 1995.

[8] Q. Wang, G. Chen, C. Zhou, R. Jin, and L. Wang, "Sacrificial template method for the synthesis of CdS nanosponges and their photocatalytic properties," *Journal of Alloys and Compounds*, vol. 503, no. 2, pp. 485–489, 2010.

[9] Y. Tak, S. J. Hong, J. S. Lee, and K. Yong, "Fabrication of ZnO/CdS core/shell nanowire arrays for efficient solar energy conversion," *Journal of Materials Chemistry*, vol. 19, no. 33, pp. 5945–5951, 2009.

[10] G. Dukovic, M. G. Merkle, J. H. Nelson, S. M. Hughes, and A. P. Alivisatos, "Photodeposition of Pt on colloidal CdS and CdSe/CdS semiconductor nanostructures," *Advanced Materials*, vol. 20, no. 22, pp. 4306–4311, 2008.

[11] C.-S. Yang, D. D. Awschalom, and G. D. Stucky, "Kinetic-dependent crystal growth of size-tunable CdS nanoparticles," *Chemistry of Materials*, vol. 13, no. 2, pp. 594–598, 2001.

[12] M. Sharma and P. Jeevanandam, "Synthesis, characterization and studies on optical properties of hierarchical ZnO-CdS nanocomposites," *Materials Research Bulletin*, vol. 47, no. 7, pp. 1755–1761, 2012.

[13] K. Yuan, L. Chen, F. Li, and Y. Chen, "Nanostructured hybrid ZnO@CdS nanowalls grown in situ for inverted polymer solar cells," *Journal of Materials Chemistry C*, vol. 2, no. 6, pp. 1018–1027, 2014.

[14] M. Zirak, O. Akhavan, O. Moradlou, Y. T. Nien, and A. Z. Moshfegh, "Vertically aligned ZnO@CdS nanorod heterostructures for visible light photoinactivation of bacteria," *Journal of Alloys and Compounds*, vol. 590, pp. 507–513, 2014.

[15] M. Misra, P. Kapur, C. Ghanshyam, and M. L. Singla, "ZnO@CdS core-shell thin film: fabrication and enhancement of exciton life time by CdS nanoparticle," *Journal of Materials Science: Materials in Electronics*, vol. 24, no. 10, pp. 3800–3804, 2013.

[16] M. Zirak, O. Moradlou, M. R. Bayati, Y. T. Nien, and A. Z. Moshfegh, "On the growth and photocatalytic activity of the vertically aligned ZnO nanorods grafted by CdS shells," *Applied Surface Science*, vol. 273, pp. 391–398, 2013.

[17] X. Wang, G. Liu, G. Q. Lu, and H.-M. Cheng, "Stable photocatalytic hydrogen evolution from water over ZnO-CdS core-shell nanorods," *International Journal of Hydrogen Energy*, vol. 35, no. 15, pp. 8199–8205, 2010.

[18] R. Wu, C. S. Xie, H. Xia, J. Hu, and A. Wang, "The thermal physical formation of ZnO nanoparticles and their morphology," *Journal of Crystal Growth*, vol. 217, no. 3, pp. 274–280, 2000.

[19] H. Park, W. Choi, and M. R. Hoffmann, "Effects of the preparation method of the ternary CdS/TiO_2/Pt hybrid photocatalysts on visible light-induced hydrogen production," *Journal of Materials Chemistry*, vol. 18, no. 20, pp. 2379–2385, 2008.

[20] J. Cao, J.-Z. Sun, J. Hong, H.-Y. Li, H.-Z. Chen, and M. Wang, "Carbon nanotube/CdS Core-shell nanowires prepared by a simple room-temperature chemical reduction method," *Advanced Materials*, vol. 16, no. 1, pp. 84–87, 2004.

[21] J. Juntaro, M. Pommet, G. Kalinka, A. Mantalaris, M. S. P. Shaffer, and A. Bismarck, "Creating hierarchical structures in renewable composites by attaching bacterial cellulose onto sisal fibers," *Advanced Materials*, vol. 20, no. 16, pp. 3122–3126, 2008.

[22] J. Z. Yang, J. Yu, J. Fan, D. Sun, W. Tang, and X. Yang, "Biotemplated preparation of CdS nanoparticles/bacterial cellulose hybrid nanofibers for photocatalysis application," *Journal of Hazardous Materials*, vol. 189, no. 1-2, pp. 377–383, 2011.

[23] C. Li, T. Ahmed, M. Ma, T. Edvinsson, and J. Zhu, "A facile approach to ZnO/CdS nanoarrays and their photocatalytic and photoelectrochemical properties," *Applied Catalysis B: Environmental*, vol. 138-139, pp. 175–183, 2013.

[24] L. Irimpan, D. Ambika, V. Kumar, V. P. N. Nampoori, and P. Radhakrishnan, "Effect of annealing on the spectral and nonlinear optical characteristics of thin films of nano-ZnO," *Journal of Applied Physics*, vol. 104, no. 3, Article ID 033118, 2008.

[25] T. K. Jana, A. Pal, and K. Chatterjee, "Self assembled flower like CdS-ZnO nanocomposite and its photo catalytic activity," *Journal of Alloys and Compounds*, vol. 583, pp. 510–515, 2014.

[26] J. Nayak, "Enhanced light to electricity conversion efficiency of CdS–ZnO composite nanorod based electrochemical solar cell," *Materials Chemistry and Physics*, vol. 133, no. 1, pp. 523–527, 2012.

[27] G. Murugadoss, "ZnO/CdS nanocomposites: synthesis, structure and morphology," *Particuology*, vol. 10, no. 6, pp. 722–728, 2012.

[28] X. Hou and L. Wang, "Sonochemical synthesis and charge transfer property of core/shell ZnO/CdS nanohybrids," *Materials Letters*, vol. 122, pp. 29–32, 2014.

[29] D. Sun, J. Yang, and X. Wang, "Bacterial cellulose/TiO_2 hybrid nanofibers prepared by the surface hydrolysis method with molecular precision," *Nanoscale*, vol. 2, no. 2, pp. 287–292, 2010.

[30] W. F. Liu, C. Jia, C. G. Jin, L. Z. Yao, W. L. Cai, and X. G. Li, "Growth mechanism and photoluminescence of CdS nanobelts on Si substrate," *Journal of Crystal Growth*, vol. 269, no. 2–4, pp. 304–309, 2004.

[31] T. Y. Zhai, X. S. Fang, Y. Bando et al., "Morphology-dependent stimulated emission and field emission of ordered CdS nanostructure arrays," *ACS Nano*, vol. 3, no. 4, pp. 949–959, 2009.

[32] W.-S. Chae, S.-W. Lee, M.-J. An et al., "Nanostructures and optical properties of mesoporous composite nanofibers containing CdS quantum dots," *Chemistry of Materials*, vol. 17, no. 23, pp. 5651–5657, 2005.

[33] S. M. Hosseini, I. A. Sarsari, P. Kameli, and H. Salamati, "Effect of Ag doping on structural, optical, and photocatalytic properties of ZnO nanoparticles," *Journal of Alloys and Compounds*, vol. 640, pp. 408–415, 2015.

[34] D.-P. Kim, C.-I. Kim, and K.-H. Kwon, "Etching properties of ZnS thin films in Cl_2/CF_4/Ar plasma," *Thin Solid Films*, vol. 459, no. 1-2, pp. 131–136, 2004.

[35] Y. Jin, Q. Cui, K. Wang, J. Hao, Q. Wang, and J. Zhang, "Investigation of photoluminescence in undoped and Ag-doped ZnO flowerlike nanocrystals," *Journal of Applied Physics*, vol. 109, no. 5, Article ID 053521, 2011.